A Survey of Active Vibration Isolation Systems for Microgravity Applications

Grodsinsky, Carlos M.[1]
Bicron Corporation, Newbury, OH. 44065
Whorton, Mark S.[2]
NASA Marshall Space Flight Center, Huntsville, AL 35812

Abstract

In view of the utility of space vehicles as orbiting science laboratories, the need for vibration isolation systems for acceleration sensitive experiments has gained increasing visibility. To date, three active microgravity vibration isolation systems have successfully been demonstrated in flight. This paper provides a tutorial discussion of the microgravity vibration isolation problem including a description of the acceleration environment of the International Space Station and attenuation requirements as well as a comparison of the dynamics of passive isolation, active rack-level isolation, and active payload-level isolation. This paper also surveys the flight test results of the three demonstrated systems: Suppression of Transient Accelerations By Levitation (STABLE); the Microgravity Vibration Isolation Mount (MIM); and the Active Rack Isolation System (ARIS).

Nomenclature

F_{act} ≡ actuator force (N)

F_{dist} ≡ disturbance force (N)

g_n ≡ non-dimensional unit of gravity ($\ddot{x}/g_o$)

---

[1] BICRON, 12345 Kinsman Rd., Newbury, OH. 44065, cgrodsinsky@bicron.com
[2] Senior Engineer,ED12/Precision Pointing Control Systems, mark.whorton@msfc.nasa.gov, Senior member AIAA

g_o ≡ acceleration of gravity (9.8 m/s^2)

d ≡ damping (Ns/m)

k ≡ stiffness (N/m)

m ≡ mass (kg)

X(s) ≡ Laplace transform of acceleration of vibratory system, s=jω (m/s^2)

X_o(s) ≡ Laplace transform of acceleration of base platform (m/^{2})

ω ≡ natural frequency (rad/s)

ω_{cl} ≡ closed loop natural frequency (rad/s)

K_a ≡ acceleration feedback gain (kg)

K_v ≡ relative velocity feedback gain (Ns/m)

K_p ≡ relative position feedback gain (N/m)

ς ≡ percent damping ratio

ς_{cl} ≡ closed loop percent damping ratio

Introduction

The orbital environment provides a unique opportunity for studying phenomena in a manner not possible on earth. An earth-orbiting spacecraft provides a low-level acceleration environment that enables microgravity (μg) science experiments in disciplines such as life sciences, materials science, combustion, fundamental physics, and fluid mechanics. As a research laboratory, the International Space Station (ISS) will exploit the near-zero gravity environment of low-earth orbit for unique state-of-the-art μg science investigations. However, due to a variety of vibro-acoustic disturbances on the ISS, the

acceleration environment is expected to significantly exceed the specifications of many acceleration sensitive experiments. Figure 1 shows the expected acceleration environment on the ISS along with the maximum magnitudes of acceptable accelerations (the ISS design requirement). Note that the requirements are most stringent at low frequencies. Although larger accelerations can be tolerated at higher frequencies, the magnitude of the ISS acceleration environment increases likewise. The ubiquity and difficulty in characterizing the disturbance sources precludes source isolation, thus requiring vibration isolation to attenuate the anticipated disturbances to an acceptable level.

The primary sources of vibration on ISS can be categorized into three characteristic frequency ranges. At low frequencies, below approximately 0.001 Hz, the dominant accelerations are caused by gravity gradients and atmospheric drag. These low frequency vibrations are determined by ISS configuration and orbit, are non-transient in nature, location dependent, and will typically be less than 10^{-5} g. At higher frequencies, above approximately 1 Hz, the vibrations are caused by sinusoidal steady-state sources such as pumps, compressors, electric motors, and fans, as well as transient sources such as impacts, astronaut motion, and higher frequency components of attitude control forces and torques. This class of vibration sources has been extensively measured on shuttle missions and will require significant isolation to meet the desired vibration goals of ISS. Because of their relative high frequency, μg experiments can be isolated from these vibrations with relatively simple (possibly passive) vibration isolation systems. The third characteristic frequency range of vibrations is the intermediate range of approximately 0.001 Hz to 1 Hz. The sources of accelerations in this range are mostly transient in nature, such as the motion of astronauts and payloads around the ISS, as well as motion of

the ISS caused by attitude control maneuvers. Because of their transient nature, the effect of these vibrations on many experiments is difficult to analyze. The calculation of resultant ISS accelerations is also complicated by the interaction of these vibration sources with the structural modes of ISS, at least at the upper end of this frequency range.

Vibration isolation for microgravity applications uniquely differs from terrestrial applications. For example, μg materials science investigations such as protein crystal growth require a quiescent environment at frequencies as low as 0.1 Hz[1], which is a significantly lower frequency range than terrestrial vibration isolation applications. To meet these frequency requirements unique instrumentation with sensitivities much greater than those used for terrestrial applications is required. Because of gravitational coupling, μg vibration isolation systems cannot be fully tested on the ground, but instead must be characterized in the orbital environment. Finally, although passive isolation techniques are often adequate to provide sufficient attenuation of vibration disturbances in the high frequency regime, isolation of low and intermediate frequency vibrations requires active isolation.

The frequency dependent nature of the vibration isolation requirement for μg science is illustrated in Figure 2 where "attenuation" is defined as the ratio of the magnitude of isolated element motion to the magnitude of base motion (acceleration or position). The derived attenuation requirement reduces the anticipated ISS acceleration level to within the required ISS acceleration levels shown in Figure 1. Just as the vibrations can be categorized into three frequency ranges, likewise three distinct frequency regions characterize the attenuation requirement. In region 1, the isolation system must

directly transmit the very low frequency quasi-steady accelerations (below 0.01 Hz) to prevent the isolated elements from bumping into the vehicle. The requirement for isolation from base motion implies that a "rattle-space" must exist around the isolated elements to allow them to remain inertially stationary with respect to the vibrating vehicle. Obviously, it is undesirable for the isolated elements to bump into the moving base since this not only negates the vibration isolation but also transmits an impulsive acceleration to the isolated element. In Region 2 between 0.01 Hz and 10 Hz, the amount of attenuation must increase one order of magnitude for every decade of frequency. Three orders of magnitude attenuation is required in Region 3 above 10 Hz.

The remainder of the paper is divided into two major sections. The first section addresses the fundamentals of μg vibration isolation with the objective of elaborating on the relative merits of passive and active isolation approaches. A comparison of the relative strengths and weaknesses of passive, active rack-level and active subrack-level isolation is presented as well. To date, three active vibration isolation systems have been flight tested on shuttle flights. These systems are the Suppression of Transient Accelerations By Levitation (STABLE) developed jointly by the NASA Marshall Space Flight Center (MSFC) and McDonnell Douglas Aerospace Corporation (MDAC), now The Boeing Corporation); the Microgravity Vibration Isolation Mount (MIM) developed by the Canadian Space Agency; and the Active Rack Isolation System (ARIS) developed by The Boeing Corporation. The final section presents an overview of flight proven vibration isolation systems with a description of current flight systems and summary results of flight data.

Micro-gravity Vibration Isolation Fundamentals

The basic objective of a vibration isolation system is to attenuate the accelerations transmitted to an isolated experiment mount either from a vibrating base or directly applied disturbances generated by the experiment. For purposes of illustration, consider a single degree of freedom dynamic system comprised of a mass, spring, and damper shown in Figure 3. Umbilicals, which pass resources such as power, data, and cooling fluids to an experiment, are the disturbance transmission path from the base to the isolated experiment ("platform"). The platform is represented by the lumped mass, m, and the umbilicals are modeled as a linear spring with stiffness, k, and a dashpot with damping coefficient, d. Base motion may be due to several sources as described in section 1, while directly transmitted forces, independent of the umbilicals, are indicated in Figure 3 by F_{dist}. These direct inertial forces may result from crew contact or payload-generated sources such as pumps, fans, motors, and structural vibration of the isolated experiment. The inertial displacement of the base is x_0 and the inertial displacement of the mass is x. An actuator used for active control is indicated by the block labeled "Act" which generates the control force F_{act}.

The response of the platform to base motion and direct inertial disturbances is given by the second order system (equation of motion)

$$m\ddot{x} + d(\dot{x} - \dot{x}_0) + k(x - x_0) = F_{dist} + F_{act} \qquad (1)$$

The transmissibility is defined as the magnitude of the transfer function from base acceleration to platform acceleration and may be obtained by taking Laplace transforms of Equation 1, resulting in

$$\frac{X(s)}{X_0(s)} = \frac{2\varsigma\omega s + \omega^2}{s^2 + 2\varsigma\omega s + \omega^2}, \tag{2}$$

where; the natural (or break) frequency is $\omega = \sqrt{\frac{k}{m}}$ and $\varsigma = \frac{d}{2\sqrt{km}}$ is the percent damping ratio. The transmissibility relates the attenuation of base motion as a function of the frequency. From Equation 2 it is apparent that the mass, stiffness, and damping terms dictate the response characteristics of the system. These discrete elements are often selected for the purpose of shaping the dynamic response of a system to provide passive vibration isolation. This response is illustrated in Figure 4 which plots the transmissibility of the second order system described by Equation 2 for varying levels of damping. This passive system behaves like a low-pass filter, transferring disturbances at frequencies below the damped natural frequency, $\omega_d = \omega\sqrt{1-\varsigma^2}$, and attenuating disturbances above ω_d. Improved isolation from base motion is achieved by decreasing the break frequency and maximizing roll-off above the break frequency, where the slope above ω_d depends on the damping. For an undamped system this slope is -40 dB/decade. Since it is typically not desirable to increase the payload mass, the break frequency may be reduced by designing the umbilicals to minimize stiffness. However, for small payload masses, achieving isolation at frequencies lower than one Hz by reducing stiffness is not possible with reasonable rattle-space constraints (± one centimeter).

A key deficiency associated with passive isolation systems is the inherent trade between resonance and high frequency attenuation. From Figure 4 note that a resonant peak occurs at the natural frequency, the magnitude of which is determined by the

damping. Greater damping results in more suppression of the resonant-amplification, albeit at the expense of reduced attenuation at higher frequencies. Thus, when selecting the parameters of a passive isolation system a design trade must be made between resonant damping and high frequency attenuation.

Another deficiency of passive isolation is rejection of inertial disturbances. To improve upon attenuation of disturbance forces applied directly to the mass with the passive system shown in Figure 3, either the platform mass must increase or a *stiff* spring must connect the platform to the base (assuming the base is sufficiently massive). Since improved base motion isolation is achieved by softening the spring connection, the objectives of base motion isolation and direct disturbance rejection are in opposition and cannot be simultaneously achieved. That contradiction between direct and base motion isolation does not arise in the case of actively controlled vibration isolation system.

Active Control Concepts

In order to provide a quiescent acceleration environment to an experiment, an active isolation system must sense and cancel the accelerations applied to the experiment. Typically a high-frequency acceleration feedback control loop is implemented to cancel the accelerations and a low frequency position feedback control loop is used to center the platform in the sway space while following the quasi-steady motion of the vehicle. By sensing relative position and absolute acceleration of the platform the active control system forces the platform to follow the very-low-frequency motion of the base while attenuating the base motion at higher frequencies. In essence, the isolation system must provide a soft suspension with respect to base motion disturbances, while providing a stiff

suspension with respect to inertial (directly transmitted) disturbances. These competing objectives cannot be attained with passive isolation, but require active isolation with inertial acceleration feedback.

To illustrate active isolation of vibrations for the single degree of freedom system in Figure 3, consider a control law using feedback of absolute acceleration, relative velocity, and relative position described by

$$F_{act} = -K_a\ddot{x} - K_v(\dot{x} - \dot{x}_0) - K_p(x - x_0) \tag{3}$$

Substituting Equation 3 into Equation 1 yields the closed-loop equations of motion:

$$(m + K_a)\ddot{x} + (d + K_v)(\dot{x} - \dot{x}_0) + (k + K_p)(x - x_0) = F_{dist} \tag{4}$$

Again, taking Laplace transforms results in the closed-loop transmissibility function

$$\frac{X(s)}{X_0(s)} = \frac{2\zeta_{cl}\omega_{cl}s + \omega_{cl}^2}{s^2 + 2\zeta_{cl}\omega_{cl}s + \omega_{cl}^2} \quad , \tag{5}$$

where; the closed-loop natural frequency is $\omega_{cl} = \sqrt{\frac{k + K_p}{m + K_a}}$ and the closed loop damping ratio is $\zeta_{cl} = \frac{d + K_v}{2\sqrt{(k + K_p)(m + K_a)}}$. Comparing the passive system with the closed-loop system indicates that the gains K_a, K_v, and K_p may be viewed as effective mass, damping, and stiffness, respectively, and may be used to modify the dynamic response of the system. For a fixed umbilical stiffness and payload mass, the break frequency can be reduced by either using positive position feedback ($K_p < 0$) to negate the spring stiffness or by using

high gain acceleration feedback (large K_a). Stiffness cancellation is not a sound approach for stability reasons and acceleration feedback is thus preferable.

Active control remedies the key deficiencies in passive isolation: direct disturbance rejection and the resonant peak/high frequency attenuation trade. Acceleration feedback is beneficial for attenuating direct disturbances by effectively increasing the dynamic mass of the isolated payload. By designing with frequency dependent gains, active control can effectively add damping in the break frequency region to attenuate the peak resonance without adversely affecting the attenuation at higher frequencies.

Vibration isolation systems are inherently multivariable systems. Cross products of inertia introduce inertial coupling in the dynamics, which can be alleviated by a proper choice of coordinate frames. However, umbilicals attached remotely from the platform center of mass introduce rotational coupling that is manifested by off-diagonal terms in the stiffness matrix. Although a coordinate transformation can be used to obtain a diagonal generalized mass and stiffness matrix, this transformation matrix is formed by the mode shapes (eigenvectors), which may not be well known. Errors in the mode shapes would manifest unmodeled coupling in the plant dynamics. Thus, for highly coupled systems, multivariable (modern) control methods may be warranted.

Performance and stability improvements can be made in some cases by using modern control techniques. Frequency weighted LQG design seeks to minimize a quadratic cost functional (an H_2 norm) that is related to the energy of the system response and the energy of the control system input. Since an objective of vibration isolation is to

minimize the mean-square acceleration of the payload, H_2 methods are well-suited for control design. [1-3]

A key shortcoming of H_2 methods is the lack of stability and performance robustness with respect to model errors. A robust control design approach for μ-g vibration isolation must account for uncertainties in umbilical properties, mass, CM location, actuator/sensor dynamics, and uncertain or unmodeled plant dynamics. Using an H_∞ norm framework, optimal controllers may be designed to provide robust stability and performance guarantees for bounded model errors. However, H_∞ control seeks to minimize the peak frequency response magnitude, which is typically not as well suited to the vibration isolation problem as the H_2 norm. H_∞ design also tends to be overly conservative for parametric uncertainty. This conservatism is somewhat lessened using μ-synthesis methods. These issues are addressed in mixed H_2/H_∞ control design which optimizes nominal performance using an H_2 norm while providing robust stability guarantees by enforcing an H_∞ norm constraint.[4] Other methods with potential applicability include adaptive and intelligent control methods. Research is currently in progress to evaluate these methods for microgravity vibration isolation applications.

Rack Isolation versus Payload Isolation

Two primary approaches are employed to provide vibration isolation for microgravity payloads. ISS management has determined that an actively controlled isolation system will be necessary to meet the requirement shown in Figure 1 and has baselined ARIS to isolate 50% of the U.S. allocation of International Standard Payload

Racks (ISPR) to be flown on ISS. STABLE and MIM provide a complementary approach to rack level isolation by providing vibration isolation directly to a payload.

The concept of isolating only the vibration-sensitive portion of a payload minimizes the number and size of utility umbilicals, which are the primary load path for vibration disturbances. Payload-level isolation is especially critical for high bandwidth control applications such as experiments with internal dynamics or forced excitation requirements. In multiple-experiment racks, a payload is isolated from disturbances produced by nearby experiments or crew servicing activities while eliminating the potential for disturbances due to accidental crew contact with the rack or its enclosure.

Possibly most importantly, sub-rack isolation allows for higher bandwidth control laws and thus better isolation performance. In order to gain stabilize the control system in the presence of uncertain structural dynamics, the control system bandwidth must be limited to the frequency range for which the dynamics are reasonably well known. The operational scenario for ARIS involves a single control system implemented on numerous racks which will be routinely modified as the contents (experiments, stowage, etc) are periodically changed out. As a consequence, the ARIS control system must be bandwidth limited in order to guarantee stability robustness, which in turn significantly limits direct disturbance rejection and forced excitation capability. With a component-level isolation system such as STABLE and MIM, the entire rack is not isolated, the uncertain rack dynamics are not a stability concern, and higher bandwidth control may be employed. Consequently, better direct disturbance rejection capability can be achieved for payloads with internal dynamics and the isolation system is able to generate user-specified excitations with greater spectral content. A key disadvantage of component-level isolation

is that a dedicated system is associated with each isolated payload thereby increasing the total cost, power, and volume utilized when compared to the cost, power, and volume required to isolate multiple payloads with a single rack isolation system.

Based on these observations, a case can be made that rack and payload level isolation systems are complementary, each being appropriate for different applications. The selection criteria primarily involve payload dynamics and the need for user-specified excitation as indicated in the design selection matrix shown in Table 1. This table suggests general guidelines for selection of the most cost-effective vibration isolation approach.

Table 1: Comparison of Isolation Approaches

Type	Advantages	Disadvantages
Passive	• Low Cost • Low Maintenance • Reliable • No Power	• Isolate only high frequencies • Large volume • Cannot mitigate self-induced vibrations • Resonance versus attenuation trade
Active Rack (ARIS)	• Low frequency attenuation • Multiple payloads isolated with one system • Standard payload interface	• Limited mitigation of payload induced vibrations • Constrains payload dynamics • Highly sensitive to crew

		contact
Active Payload-Level (STABLE, MIM)	• Low frequency attenuation • Mitigates payload induced vibrations • Optimized for individual payload	• Single payload per unit (more resources)

Flight Proven Micro-gravity Vibration Isolation Systems

Much work has been done during the past decade toward the development of active isolation systems for μg payloads. The NASA Lewis Research Center (LeRC) conducted an Advanced Technology Development Project in Vibration Isolation Technology from 1987 through 1992, which sponsored in-house technology and funded numerous contractor studies and hardware development.[5] A six degree-of-freedom (DOF) laboratory testbed was developed to evaluate concepts and control strategies leading to an aircraft testbed system that was successfully tested on the NASA LeRC Learjet.[6] Based on two decades of experience in active suspension systems, the Honeywell Corporation (formerly Sperry) developed the first isolation system for space shuttle flight applications called the Fluids Experiment Apparatus Magnetic Isolation System (FEAMIS) to support Rockwell's Fluid Experiment Apparatus (FEA).[7] However, FEAMIS was never flown. An isolation system was developed by the European Space Agency, also called the Microgravity Isolation Mount (MGIM), and tested in the

laboratory to support Space Station research.[8] Similarly, Satcon Corporation developed a ground test version of a 6-DOF-vibration isolation system.

To date, three active vibration isolation systems have been flight tested on shuttle flights. The STABLE (Suppression of Transient Accelerations By Levitation) μg vibration isolation system was the first to be flown in space on STS-73/USML-02 in October 1995. STABLE was developed jointly by the NASA Marshall Space Flight Center (MSFC) and McDonnell Douglas Aerospace Corporation (MDAC, now The Boeing Corporation). Shortly thereafter, the Microgravity Vibration Isolation Mount (MIM) developed by the Canadian Space Agency began operation aboard the Russian MIR space station during April 1996 and was flight tested on the space shuttle flight STS-85 in August, 1997. The Active Rack Isolation System (ARIS), developed by The Boeing Corporation was flight tested on STS-79 in September 1996.[9] The following sections provide an overview of these three flight systems with a summary of data from their respective flights.

STABLE Overview

In early 1995, MSFC teamed with MDAC to jointly develop a μg vibration isolation system called STABLE. This effort culminated in the first flight of an active μg vibration isolation system on STS-73/USML-02 in late 1995. Beginning with an authorization to proceed in mid-January 1995, the schedule required delivery of flight hardware to the NASA Kennedy Space Center during the first week of June 1995. This aggressive schedule required design, analysis, fabrication, procurement, integration, testing, and delivery of qualified flight hardware in less than five months. To meet this schedule, the STABLE project team utilized available hardware (including field-tested

actuators) and electronics to build the isolation system without procuring long lead-time items. A very robust control design philosophy was required due to the lack of a high fidelity control design model. A more complete description of STABLE and an analysis of flight data are given in Ref. 10.

STABLE Hardware Description

STABLE provides component-level isolation as an alternative to the rack-level approach of ARIS. Both STABLE and a fluid dynamics experiment dubbed "CHUCK" were contained within a single middeck locker. As shown in Figure 5, STABLE is comprised of a middeck locker, an isolated platform on which CHUCK is mounted, three actuator assemblies, nine acceleration sensors, three position sensors, and the associated electronics and control boards. Three electromagnetic actuators developed by Boeing (formerly MDAC) suspend the platform from the base of the locker box. The only physical connections between the isolated platform and the base are the flexible umbilical cables that provide power and data to and from the platform. A lockdown mechanism is used to secure STABLE during launch and reentry.

Each actuator assembly provides two axes of force with a gap that allows +/- 1 cm of travel in each axis. A high bandwidth acceleration feedback control loop and a low bandwidth relative position feedback control loop are implemented to produce the required control force in each actuator force axis. Six accelerometers and three relative position sensors are used to sense the isolated platform motion. The accelerometers are mounted in pairs on each of three mounting brackets oriented to measure acceleration

along the actuator force directions. Three additional accelerometers mounted to the back of the locker box provide a measure of the non-isolated indirect disturbance environment. AlliedSignal model QA-2000 proof-mass accelerometers are used on both the platform and base. Each of the three position sensors measure relative position of the platform with respect to the base in two orthogonal axes using a laser illuminator mounted on the platform and a photo-resistive detector fixed to the base.

STABLE Control Algorithms

The key to the robustness of STABLE is its six independent position and acceleration loops based on the co-location between sensors and actuators. The low bandwidth digital position controller uses measurements from the position sensors to compute the six-degree-of-freedom (6-DOF) displacement of the floating platform and keep it centered in its "rattle-space" over a period of minutes. Each acceleration loop is closed through an analog controller with approximately a 50-Hz bandwidth to null the sensed acceleration of the platform. A block diagram of this system is shown in Figure 6.

A digital proportional-integral-derivative (PID) controller is implemented for position control along each actuator axis. The position control law operates in one of two modes, high gain or low gain, depending on the calculated actuator gap. Integral control is used to compensate for the accelerometer bias calibration error, unknown umbilical bias force, and accelerometer bias drift due to temperature variations. Acceleration commands in each actuator input axis are computed by the position control law and are summed with the accelerometer signals to form the error signal which is the input to the acceleration loop control law.

The analog acceleration controller attempts to mitigate platform acceleration disturbances sensed by the accelerometers using rate feedback for stability robustness. A low-pass filter provides roll-off at a nominal bandwidth of 50 Hz. Since analog controllers are impervious to single-event upsets (SEUs) caused by radiation while in orbit, the STABLE analog acceleration system is less likely to suffer upsets than the ARIS or MIM digital control systems. Analysis shows that the STABLE analog acceleration controller would suffer a single-event upset once every 27 years.

STABLE Flight Data

The STABLE flight demonstration recorded measurements of the isolated payload's acceleration and position, base (ambient) acceleration levels, actuator currents, accelerometer temperature, and control system gain settings and parameters to be utilized for system performance evaluation. In addition, thermal and video data from the science payload were obtained. STABLE was designed for autonomous operations with minimal astronaut attention, little ground communication, and no data telemetry. A 486-laptop computer with two 12-bit analog-to-digital PCMCIA cards was used as a data acquisition system for the on-orbit measurements. After activation of STABLE and the laptop, measurements were recorded to a RAM disk, which was periodically copied on to the laptop hard drive. Each hard drive held about 12 hours of data and a total of about 72 hours of data was recorded on-orbit. The data acquisition system sampled and recorded acceleration and actuator current data at a rate of 250 Hz. Position and temperature data was sampled at 10 Hz.

The three translational components of acceleration from the middeck locker frame and experiment platform were processed to yield a variety of isolation system performance measures. These measures included time history, RMS, histogram, power spectral density, cumulative power spectral density, transfer function, and one-third octave integrated power spectrum (RMS average over a small frequency band). The one-third octave integrated power spectrum plot is used to compare STABLE performance with the current ISS program requirements.

The data presented here are from a crew exercise period, which yielded the most significant force levels recorded by STABLE. A key time-domain performance indicator is the acceleration time history shown in Figure 7. The ambient vibration levels of the shuttle are attenuated by a factor of 26.7 on the STABLE isolated platform. Transient peak accelerations greater than 800 μg are measured on the base, while the isolated platform acceleration peaks are below 40 μg. With an root-mean-square (RMS) base acceleration of 165.7 μg for this time period, the RMS value of the attenuated platform acceleration was 6.2 μg. The frequency domain data presented in Figure 8, from the previous time histories, were processed using standard windowing and averaging techniques. The total time history for each data block was separated into 20 ensembles, adjusted to zero mean, and windowed using the power-corrected Hanning method before transformation into the frequency domain. Fast Fourier transforms were performed with 16384 points, yielding spectral data down to 0.015 Hz. As a check, total power in the time and frequency domain signals was compared and verified to be essentially the same.

The frequency domain performance of STABLE is illustrated in Figure 8, which presents the power spectral density curves integrated over one-third octave frequency

bands with the square root taken of the resulting integral to reduce the units to mg. Figure 8 shows that STABLE performed well across a wide frequency spectrum. During this microgravity science mission, the Orbiter environment was significantly more quiescent than the anticipated ISS environment shown in Figure 1. The Orbiter environment met the ISS design requirement in all frequency bands except for one in this time history (which was the worst case in measured data). However, the shuttle is not expected to have significant disturbances in the frequency band below 1 Hz. Nonetheless, the ambient acceleration is significantly attenuated across all frequencies above approximately 0.03 Hz where the STABLE attenuation begins. The isolated platform results shown in Figure 8 represent not only platform motion but include the contribution of accelerometer noise and noise due to aliasing and quantization. Hence, the actual platform motion is less than that shown in the isolated curve. A higher sampling rate and better filter choices would have provided further improvement.

Taking the ratio of the RMS values of on-board acceleration to off-board acceleration in one-third octave bands at data points of high correlation, the attenuation function shown in Figure 9 results. Note that the break frequency occurs at approximately 0.03 Hz and the high frequency roll-off is approximately -20 dB per decade up to around 10 Hz (above which the signal was below the sampling resolution). Although this attenuation function has a slightly higher break frequency than the requirement shown in Figure 2, it should be noted that the schedule allowed no time for control system optimization and hence a robust control system was implemented at the expense of sacrificing isolation performance. These results do not indicate the limiting performance attainable by STABLE.

Considering the four and one-half month schedule, STABLE operated quite successfully. Based on examination of flight data, the STABLE isolation system was able to provide substantial attenuation of disturbances on board the shuttle. Acceleration levels were reduced by an order of magnitude or more over the desired frequency range.

MIM Overview

The Microgravity Vibration Isolation Mount (MIM) was developed by the Canadian Space Agency (CSA). The MIM device is also a component-level acceleration feedback based active isolation system. The first MIM unit was developed and launched by CSA as a NASA payload on the Priroda laboratory module, which docked with the Russian Mir space station in April 1996. The first MIM system was operated on the Mir from May 1996 to January 1998, accumulating more than 3000 hours of operation supporting several fluid physics experiments. An upgraded system (MIM-2) was flown on STS-85 in August 1997. The major improvements to the MIM-2 in comparison to the original MIM are in the design of the electronics and the actuators. The MIM system is a middeck locker type design, which interfaces to an experiment through a tabletop interface. Figure 10 shows the isolation platform and its experiment interface. The MIM design also provides the experiment user an ability to provide controlled acceleration inputs in order to assess g-jitter sensitivity parameters for specific experiment phenomena. The STS-85 MIM-2 flight's primary objectives were to test its isolation performance with and without the controlled excitation and to examine the effects of g-jitter on certain fluid physics experiments. This paper will only summarize the isolation performance of the MIM system as configured for the STS-85 flight and reported in References 11 and 12.

MIM Control Algorithms

The MIM-2 performance tests were run with a number of different control algorithms. In all cases, the algorithms incorporated dual or mixed control loops using relative position, payload orientation, and acceleration measurements as control states. As in the G-limit design the control of the isolated platform is based on six degree-of-freedom magnetic levitation utilizing eight wide gap Lorentz force actuators. The system includes three light emitting diodes imaged onto three two axis light sensing devices, which allow position and orientation tracking of the platform relative to its base. The system also includes six accelerometers for monitoring the base and isolated platform. The three platform accelerometers are also used for the acceleration feedback control states.

A number of different controllers were investigated as part of the STS-85 mission objectives. Various optimal control strategies were used as well as classical PID algorithms. All of the control laws used the inertial states of the platform as control states. The control algorithms investigated included a dual PID scheme (DPID), a pole placement design using a Q-factorization scheme (QP), a digital pole placement in the RST format (RST), an H_2 optimization scheme and an H_∞ optimization scheme. These control algorithms were the result of a number of researchers.[11]

The MIM is designed to provide isolation above 0.01 Hz. Above the control bandwidth, the system provides passive mechanical isolation. In addition to providing an attenuated environment, the system can inject known disturbances with well-controlled acceleration levels. These direct disturbances can be from several micro-g to 25 milli-g

levels in the 0.01 to 50 Hz frequency range, constrained by the 1-cm sway space. The MIM control software has the ability to generate a wide range of time histories depending on individual experiment needs. This ability to generate controlled disturbances provides investigators the ability to explore experiment parameter g-jitter sensitivities. Of course, these disturbances may be detrimental to adjacent experiments and must be accounted for as part of a disturbance allocation budget for any microgravity research facility.

MIM Flight Data

The MIM attenuation is demonstrated by comparing the acceleration time history of the stator and flotor X-axes in Figure 11. Figure 12 shows the flotor acceleration time history. These plots indicate a reduction of peak accelerations from 2500 μg on the stator to less than 50 μg on the flotor.

The system closed loop control bandwidth was designed to be between 0.01 to 100 Hz where the acceleration loops are rolled off after approximately 25 Hz. It was found early in the STS-85 mission that the MIM system did not exhibit the closed loop low frequency performance expected. The response below 1.5 Hz did not center the isolated platform as designed. The cause of this response was the attraction between the magnets providing the magnetic field for the actuator coils, and the ferromagnetic casing enveloping position sensors attached to the base. This non-linear attractive force caused the system to have non-linear negative spring rates in certain directions of motion. Due to this problem, the controllers were redesigned to provide a 0.3-Hertz cut-off frequency in the Z-axis or perpendicular to the platform. The cut-off frequency in the other axes was

set high enough to maintain a separation between the magnets and the position sensing devices.

Power spectral densities and transfer functions were calculated from time histories taken during the STS-85 mission. The spectral responses were calculated by averaging over 8-second time windows providing a spectral resolution slightly greater than 0.1 Hz. The following performance spectra and transfer functions were the result of the digital pole placement control algorithm. Figure 13 shows the power spectral densities (psd) for the platform and middeck locker interface to the MIM. At lower frequencies the platform tracks the shuttle accelerations, while at frequencies above the closed loop cut-off the platform accelerations are attenuated until the accelerometer noise floor and/or quantization resolution is reached. Figure 14 shows the transfer functions calculated from the two-psd curves in Figure 13. The leveling of the transfer functions between 30 to 100 Hz demonstrates the system approaching the accelerometer noise floors, while the anti-aliasing filters cause the change in slope above 100 Hz. The signals are rolled off with fourth order Butterworth filters above 100 Hz. The MIM-2 system's accelerometer noise floor is documented at 0.1 $(\text{micro-g})^2/\text{Hz}$ above 20 Hz with an acceleration resolution of 1 micro-g. This system noise floor performance is illustrated in the platform response psd curves of Figure 13.

ARIS Overview

The basic Active Rack Isolation System (ARIS) concept was derived through on-going developments from several international programs and findings made by NASA's Advanced Technology Development (ATD) Vibration Isolation Technology (VIT)

project. Boeing pursued the active magnetic isolation technique and focused on providing isolation for the ISPR payloads. Since predictions revealed that the station acceleration environment could be as much as 10 times higher than acceptable levels NASA base-lined ARIS in order to provide ISS with an acceleration environment as defined in the ISS Microgravity Environment Specification[13].

Of the three systems, ARIS is the only rack-level isolation system. Detaching the individual payload racks from the station structure allows the racks to be held inertially fixed by an active control system that applies inertial forces at the station to rack interface (through the ARIS actuator pushrods). These ARIS racks are dynamically controlled by closing feedback loops around inertial sensors and voice coil rotary actuator/pushrods, which connect the rack and station structure. Umbilicals are connected from the Station structure to the rack in order to support power, fluid cooling, and data communication as required by the science payloads. The undesirable accelerations transmitted through the reaction forces of the umbilicals and the actuator pushrods are reduced by the active isolation system.

The ARIS hardware configuration is shown in Figure 15. The inertial motion of the rack is measured using two tri-axial and one bi-axial accelerometer heads located in the rack. Hard stop bumpers are incorporated into the rack-station interface structure to constrain the rack so as not to exceed the ±0.5-inch sway space limit and prevent the isolated rack from bumping into station structure.

The primary objective for ARIS is to meet the isolation requirement shown in Figure 1. The formulation of this requirement was based on Station acceleration

environment predictions and the science microgravity requirement. The Risk Mitigation Experiment (RME) 1313 was flown in a modified Spacehab rack on the Mir Spacehab STS-79 mission in 1996. The objective of the ARIS flight experiment was to demonstrate that this design approach satisfied the isolation requirement.

ARIS Control Algorithms

The ARIS control algorithms are executed by a digital controller located in the bottom of the ARIS rack. Low authority position feedback is blended with the acceleration feedback to keep the rack away from station structure so that ISS structural vibrations may be isolated without impact interruptions. Kinematic and dynamic decoupling is used to account for mass properties of the integrated payload, the stiffness properties of the umbilicals, and the skewed locations of the actuators and sensors. Decoupling is also used to formulate a single-input-single-output control approach by resolving and compensating the translational and rotational motion of the rack.[9]

The ARIS control block diagram is illustrated in Figure 16. ISS motion transmits disturbance forces to the rack through the umbilicals and actuator linkage while payload equipment and lab acoustics apply direct forces to the rack. The controller also applies disturbance forces to the rack in response to the accelerometer and position sensor noise and measurement errors. The control algorithm is based on rack inertial acceleration and relative position feedback, umbilical stiffness cancellation, anti-bump compensation, and sensor-to-rack and control-to-actuator coordinate transformation matrices. The acceleration and relative position control loops each consist of six independent classical (single-input, single-output) control laws, one for each rigid body degree-of-freedom. In

order to guarantee stability and performance of the closed loop system, the dynamics must be sufficiently decoupled. Rigid body dynamic decoupling is accomplished through a transformation of the acceleration and position measurements to a body fixed coordinate frame shown in Figure 15. The transformation matrices shown in the block diagram are derived from the sensor and actuation configurations and the reference frame used to resolve the six rigid-body control directions with the origin at the integrated rack center-of-mass. Because of the large offset of the umbilical attach point (at the base of the rack) from the origin of the platform coordinate system, significant umbilical stiffness coupling occurs, resulting in large off-diagonal terms in the stiffness matrix. The mass and stiffness decoupling matrices were added in order to remedy this coupling of rotational and translational motion. A "stiffness cancellation" approach is employed which attempts to effectively diagonalize the stiffness matrix and reduce the diagonal elements to the design value by relative position feedforward control. Any measurement and/or non-linearity errors will limit the amount of decoupling one can achieve. The ability to identify and compensate for mass and stiffness properties will directly impact the achievable control response performance and stability margins.

ARIS Flight Data

A number of data sets were taken during the flight. The flight test plan was to incorporate a number of test runs with minimum and ISS full configuration umbilical sets. Due to difficulties during the flight experiment and a push rod failure the ISS umbilical configuration was never fully run. The following data given in Figure 17 show a quiescent test where the Shuttle was docked to Mir with no thruster firings and while the crew was

sleeping. The anti-bump routine was off and a 21 minute and 20 second data set was taken. In addition, the acceleration levels during crew exercise are shown for both the off-board and rack attenuated accelerations during a 14-minute crew exercise period. The ARIS calculated attenuation at the rack center-of-mass is given in Figure 18 for this data as well as for one of the accelerometer head locations with the least attenuation performance.

From 0.04 to 0.4 Hz the calculated center-of-mass attenuation was about 6 dB higher than the performance requirement. This response in the 0.04 to 0.4 Hz range was attributed to a non-linear hysteresis of the umbilical set during small amplitude motions. Consistent with the VIT ATD findings, umbilical stiffness non-linearity most significantly effects the performance of these active isolation systems. Quantization and system noise floor levels are limits as to the quiescent performance but are currently not the limiting factors.

Conclusions

As described in the previous text, achieving the microgravity requirement on the ISS will require a multifaceted solution. Both rack and sub-rack level isolation approaches have merit; the appropriate design solution depending on individual experiment and general NASA microgravity research requirements. The fundamental active inertial isolation solution has been reviewed demonstrating the basic differences between simple passive and both active suspension and inertial payload control approaches. In summary, if a payload is not sensitive to the lower frequency disturbances a simple passive suspension approach will be the most cost effective and robust isolation

solution. However, if lower frequencies are of concern and one has a dynamic experimental payload which could be causing self induced disturbances an active inertial isolation approach is dictated.

To date three systems have been flown in-orbit demonstrating the utility and design of active inertial isolation approaches. Two systems, STABLE and MIM are sub-rack level systems while the ISS vehicle solution for the general microgravity requirement is a rack level design. As was stated and investigated through NASA's VIT ATD program and other research projects, the performance limits on these systems are dictated by quantization errors, sensor noise floor, and both plant mass and umbilical stiffness and damping matrices.

The evolution of the ISS design has led to potential limitations on long-term, low-gravity experimentation in this environment and prompted the vehicle to adopt the current microgravity requirement for the US laboratory module. Many of the microgravity experiments currently supported through CODE UG and ESA will require isolation from the station random milli-g environment if reproducible and useful results are to be expected. The active isolation approach offers significant advantages over passive systems in the orbital acceleration environment. This is due to the extremely small dynamic stiffnesses needed to isolate against such low frequency base disturbances and the added capability to adapt to direct disturbances. In addition, since the responses to these two excitations require conflicting solutions a closed loop system is dictated for the control of both types of excitations.

Active systems require sensing of motion and position, and a feedback control loop to counteract mechanical excitation and minimize motion of an isolated body. Such systems introduce the complexity of a high-gain control system, but offer significant advantages in versatility and performance in the expected ISS environment.

References

1. Knospe, C. R., Hampton, R. D., and Allaire, P. E., "Control Issues of Microgravity Vibration Isolation," *Acta Astronautica*, Vol. 25, No. 11, 1991, pp. 687-697.
2. Hampton, R. D., Knospe, C. R., and Grodsinsky, C. M., "Microgravity Isolation System Design: A Modern Control Synthesis Framework," *Journal of Spacecraft and Rockets*, Vol. 33, No. 1 1996, pp. 101-109.
3. Hyde, T. T, and Crawley, E. F., "H_2 Synthesis for Active Vibration Isolation," *Proceedings of the American Controls Conference*, Seattle, WA, June 1995.

"DO we know the editor and pages from the publication. The reviewer wanted this."

4. Whorton, M. S., "High Performance, Robust Control of Flexible Space Structures," Ph.D. Dissertation, The Georgia Institute of Technology, Aug. 1997. (Also NASA TM 1998-207945, May 1998)
5. Lubomski, J. F., Grodsinsky, C. M., Logsdon, K. A, Rohn, D. A., and Ramachandran, N., "Final Report-Vibration Isolation Technology (VIT) ATD Project," NASA TM 106496, March 1994.

6. Grodsinksy, Carlos M., "Microgravity Vibration Isolation Technology: Development to Demonstration," Ph.D. Dissertation, Case Western Reserve University. (Also NASA TM 106320, Sept. 1993)

7. Allen, T. S., Havenhill, D. D., and Kral, K. D., "FEAMIS: A Magnetically Suspended Isolation System for Space-Based Materials Processing," 1986 AAS Guidance and Control Conference, Keystone, Colorado, Feb. 1-5, 1986"Whants AIAA paper #".

8. Owen, R. G.., Jones, D. I., and Owens, A. R., "Mechanical Design and Simulation of a Microgravity Isolation Mount for Columbus," *Journal of Spacecraft and Rockets*, Vol. 30, No. 4, July-August 1993.

9. Bushnell, G. S., and Becraft, M. D., "Microgravity Performance Flight Characterization of an International Space Station Active Rack Isolation Prototype System," Proceedings of The 16th IEEE Instrumentation and Measurement Technology Conference (IMTC/99), Venice, Italy, May 24-26, 1999 "Wants editor"

10. Nurre, G. S., Whorton, M. S., Kim, Y., Edberg, D. L., and Boucher, R., "Performance Assessment of the STABLE Microgravity Vibration Isolation Flight Demonstration," submitted for publication to *Journal of Spacecraft and Rockets*.

11. Tryggvason, B. V., Stewart, B. Y., and DeCarufel, J., "The Microgravity Vibration Isolation Mount: Development and Flight Test Results", IAF Paper No. IAF-97-J.2.04.

12. Canadian Space Agency, "Microgravity Vibration Isolation Mount (MIM)," Released Nov. 7, 1997. Maybe we lose this reference I do not think we can give and identification

13. Boeing Defense & Space Group Missiles and Space Division, "System Specification for the International Space Station," Specification #41000D, Nov. 1, 1995.

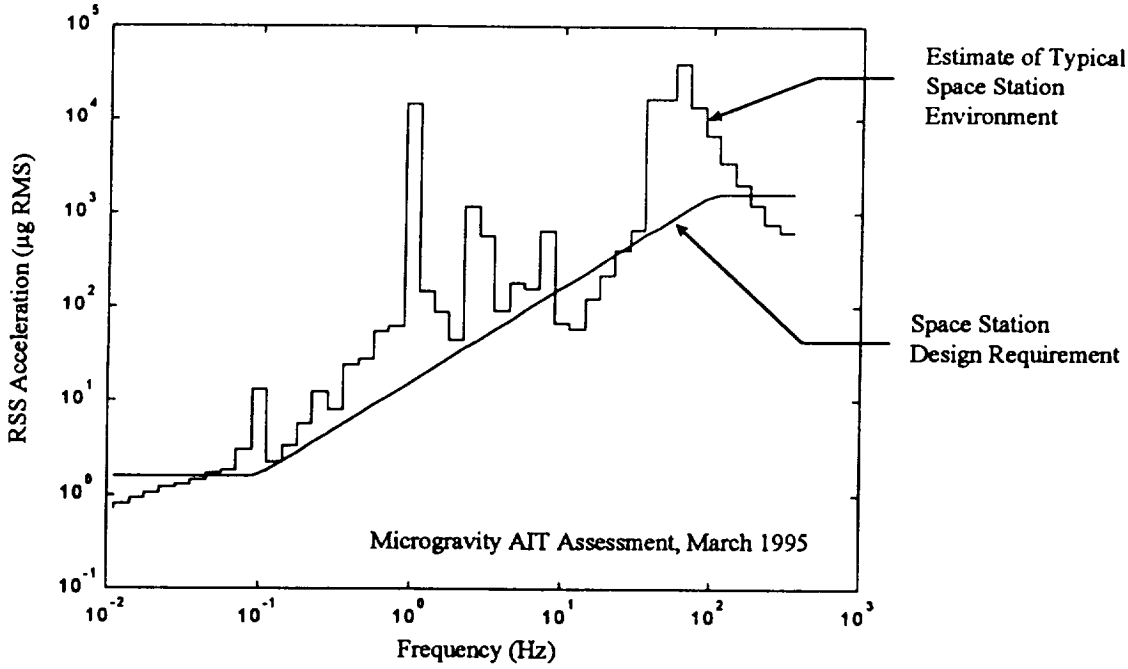

Figure 1. Microgravity Acceleration Requirements

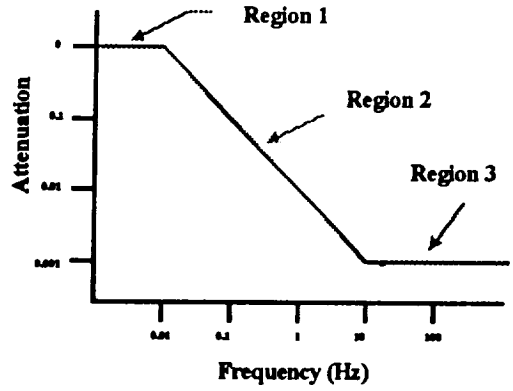

Figure 2. Microgravity Isolation System Attenuation Requirements

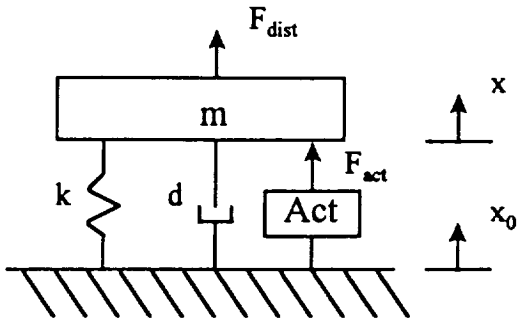

Figure 3. One Degree-of-Freedom Example

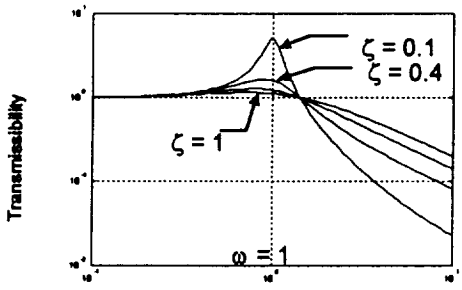

Figure 4: Transmissibility of Second Order System

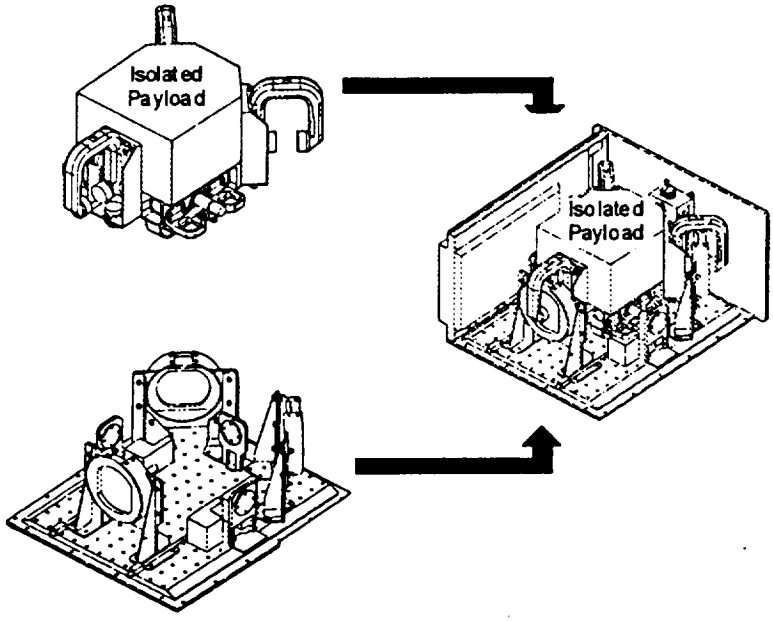

Figure 5: The STABLE Vibration Isolation System

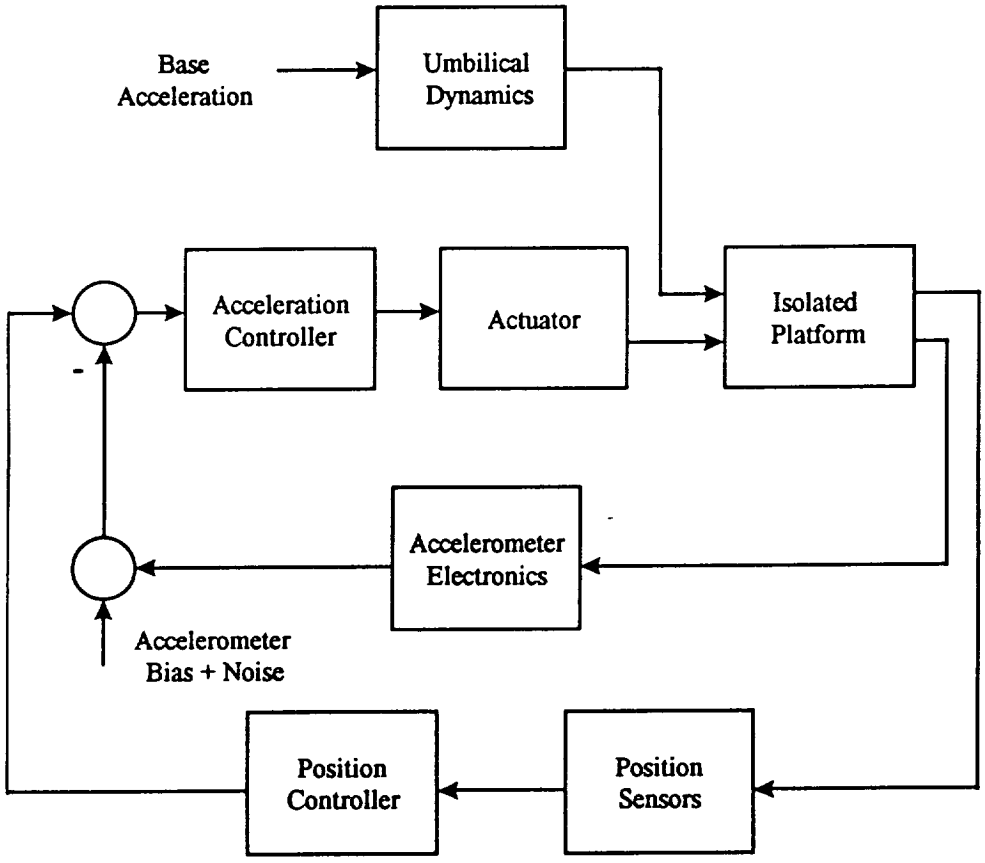

Figure 6: STABLE General Block Diagram

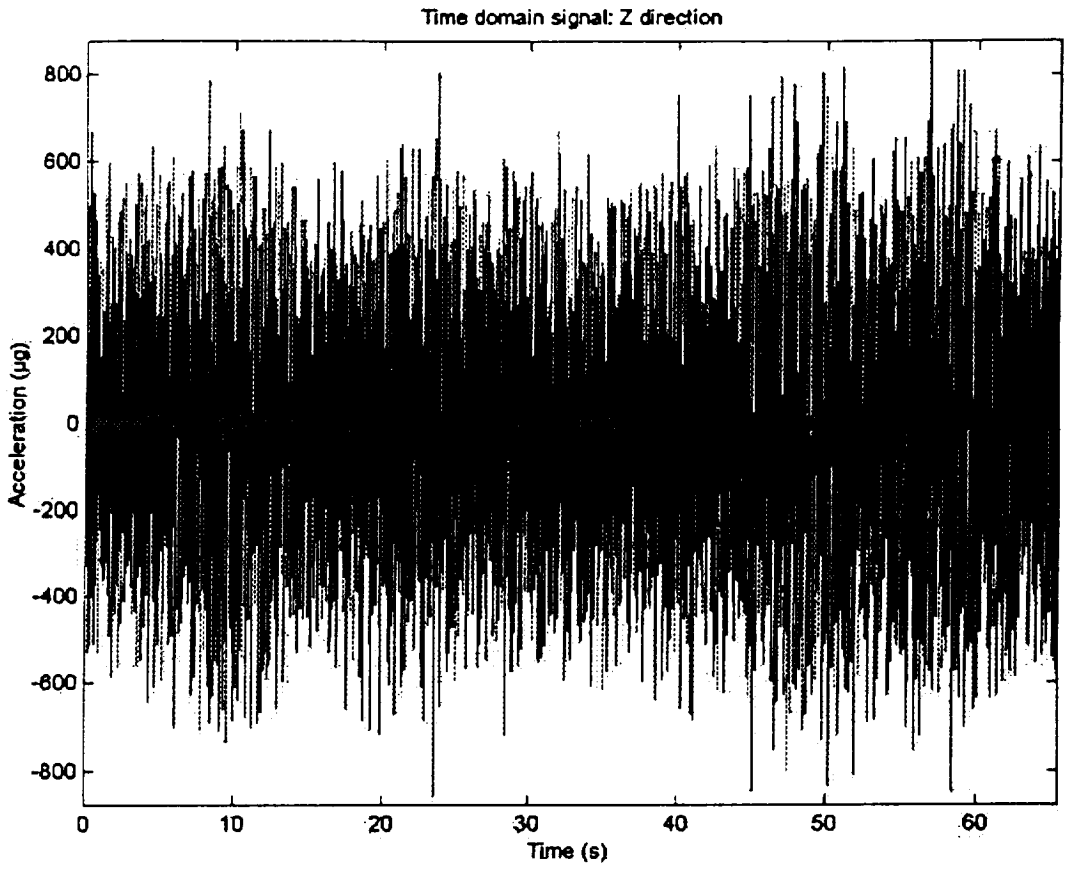

Figure 7: Shuttle and STABLE Time History during Crew Exercise

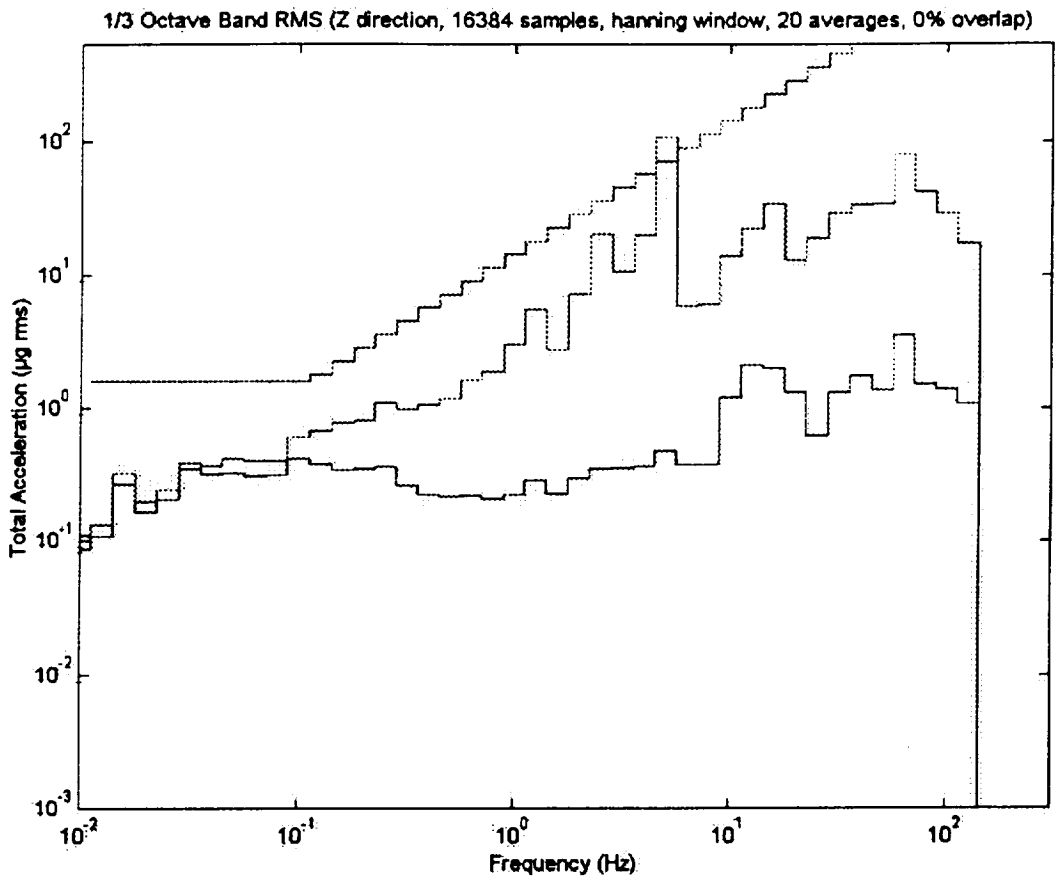

Figure 8. STABLE Acceleration 1/3 octave band measurements During Crew Exercise

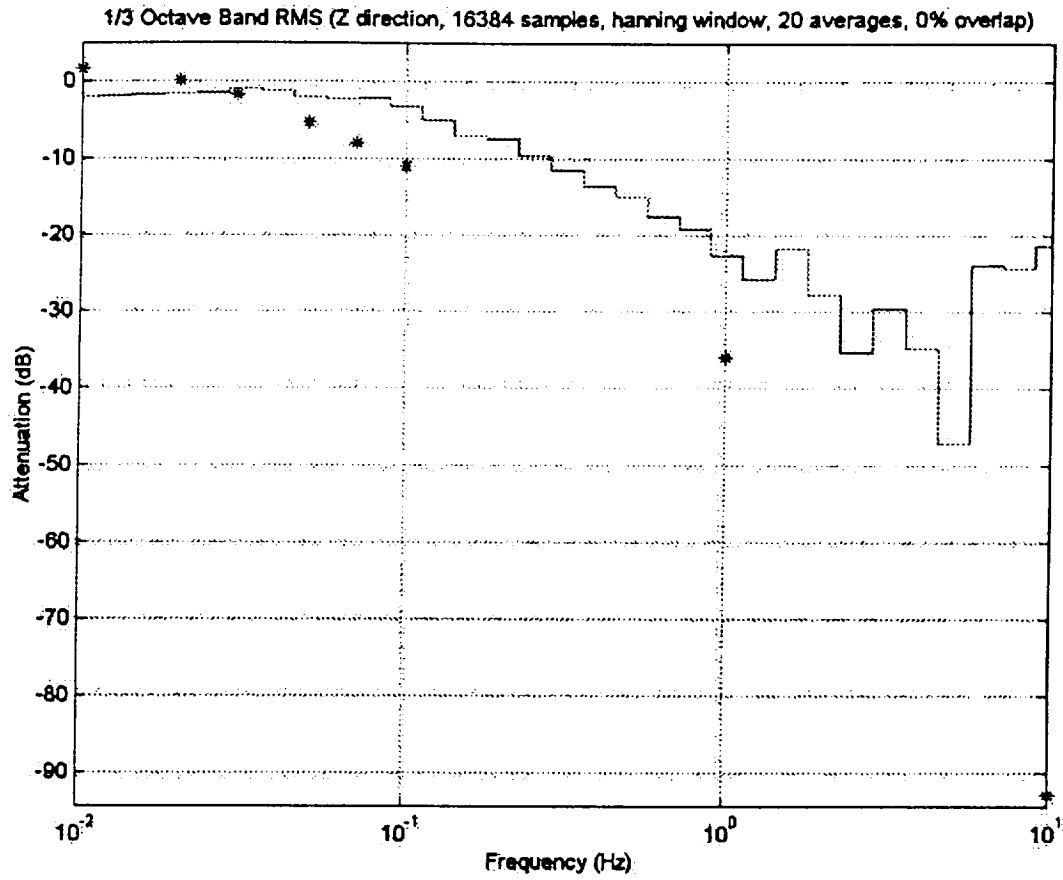

Figure 9: STABLE Attenuation Function

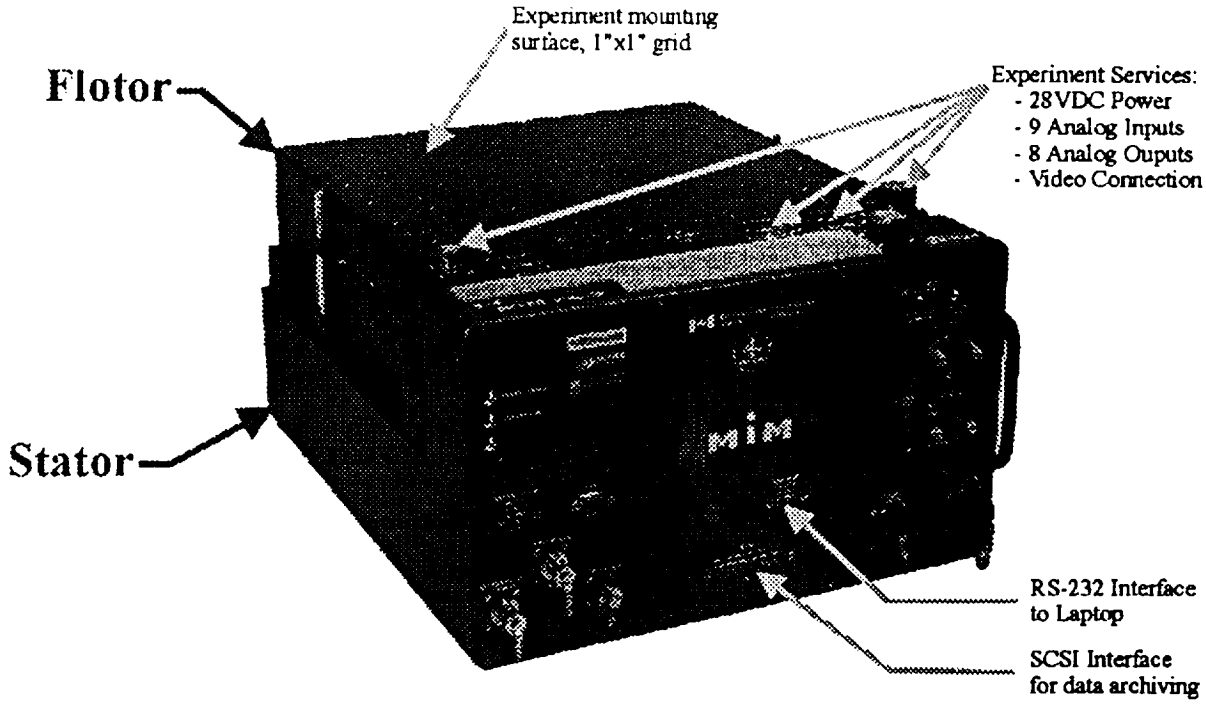

Figure 10: MIM envelope.

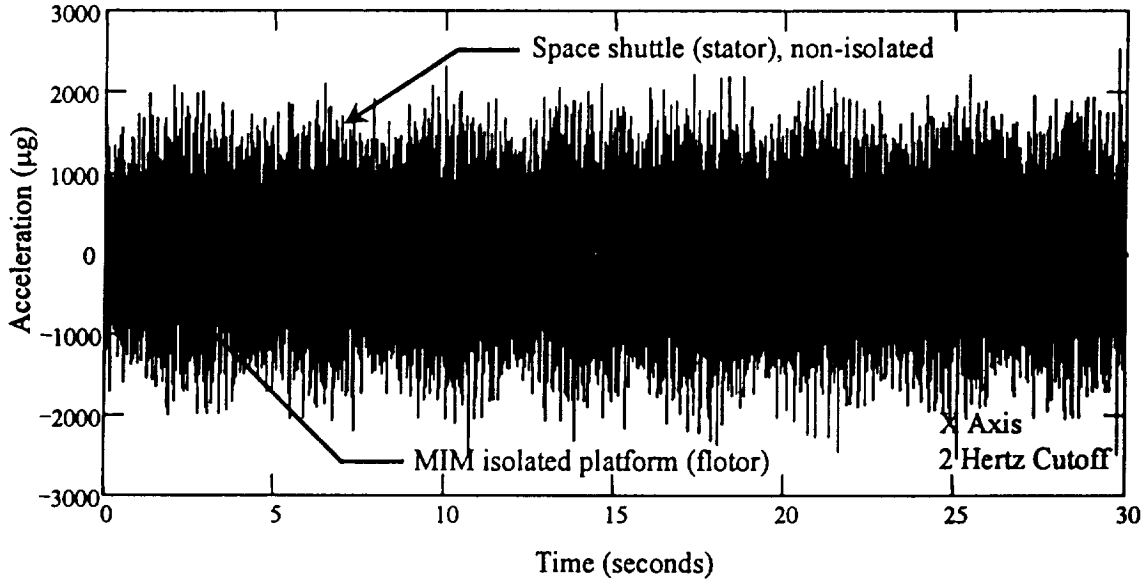

Figure 11: Example of the Acceleration Time History for the Shuttle and MIM-2 Flotor With the Isolation Cutoff Frequency Set to 2.0 Hz

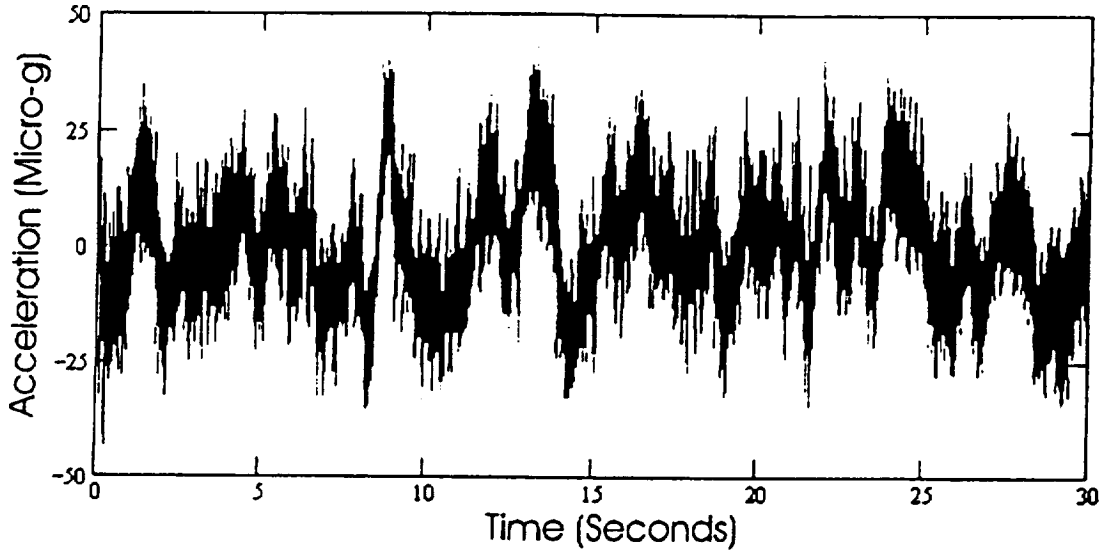

Figure 12: MIM Flotor X Acceleration Time History

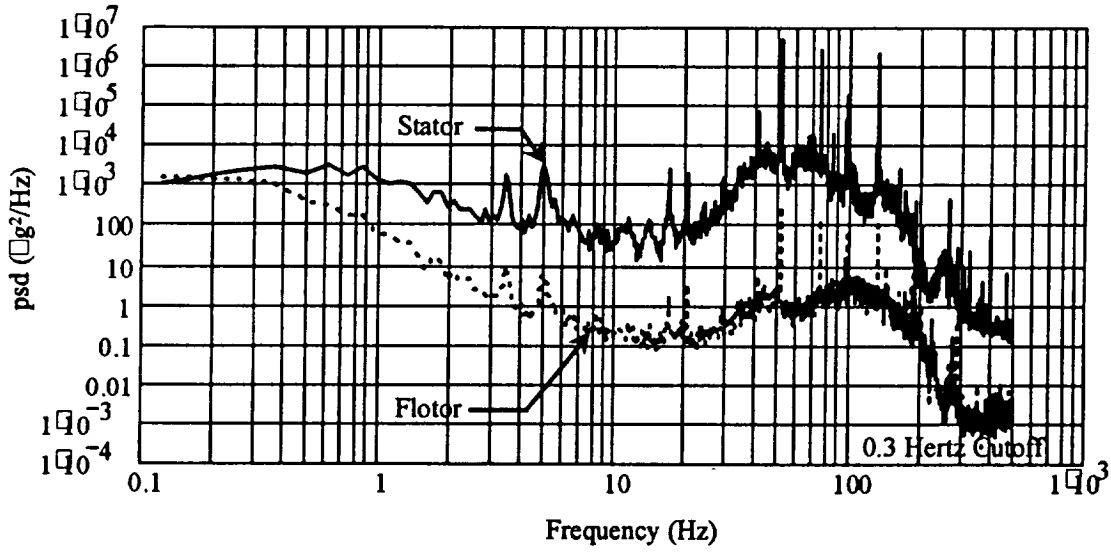

Figure 13: Power Spectral Densities for Accelerations in the Vertical Direction of the Shuttle (Stator) and the MIM-2 Flotor with the Isolation Cutoff Frequency Set to 0.3 Hz

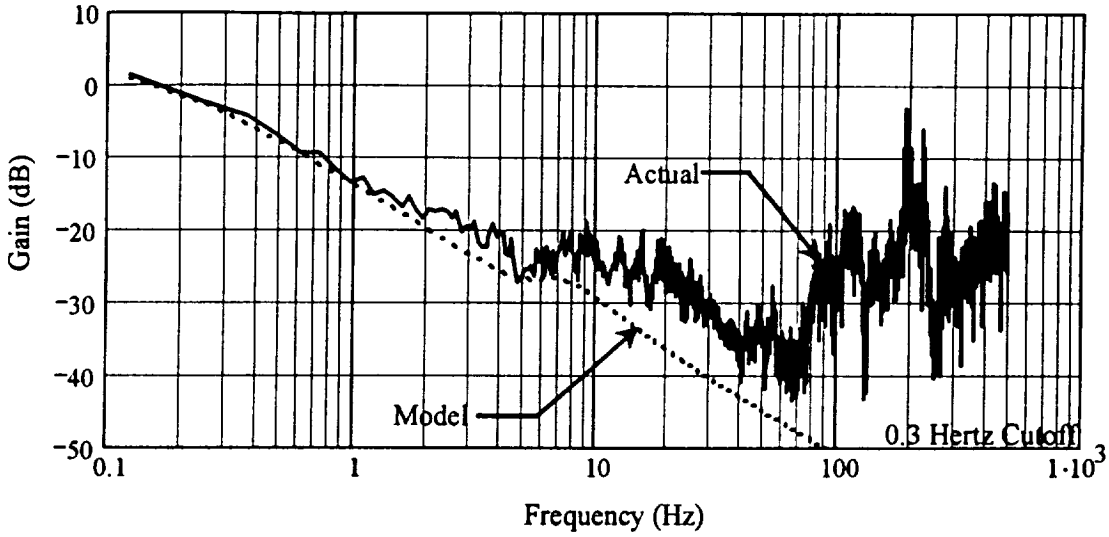

Figure 14: Transfer Function Gain for the Vertical Direction with the Cutoff Frequency Set to 0.3 Hz

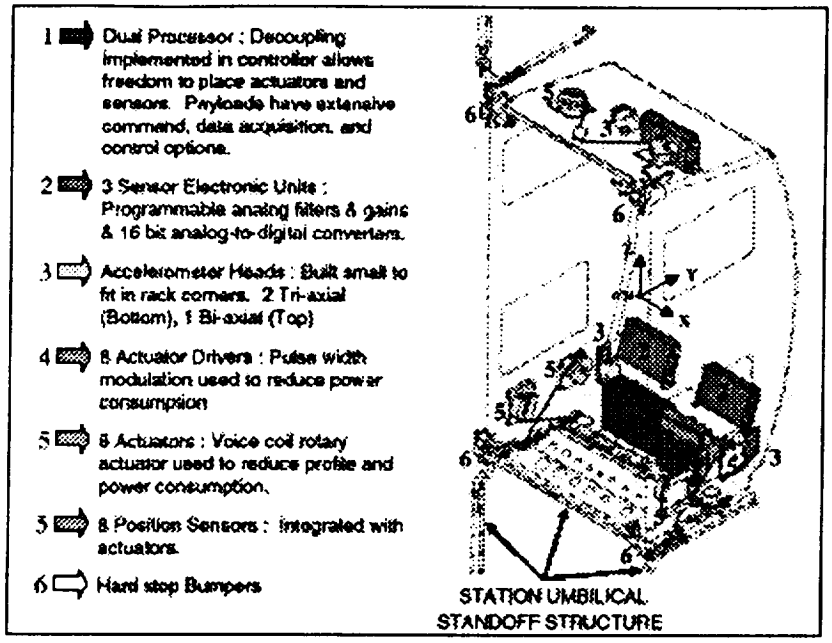

Figure 15: ARIS Hardware Configuration.

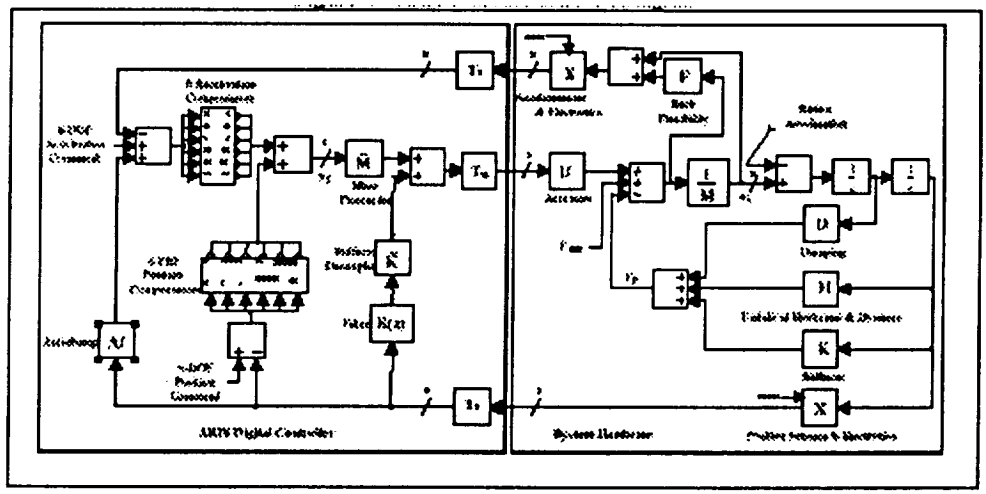

Figure 16: ARIS functional control block diagram.

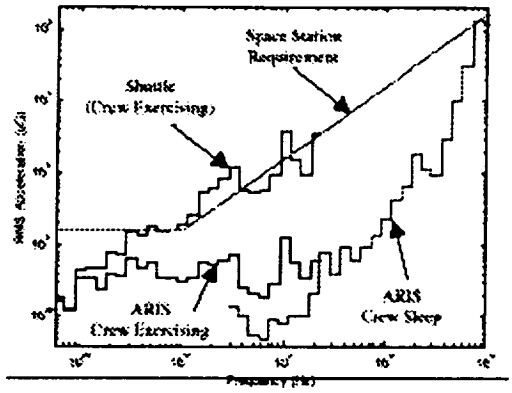

Figure 17: ARIS acceleration 1/3 octave band measurements.

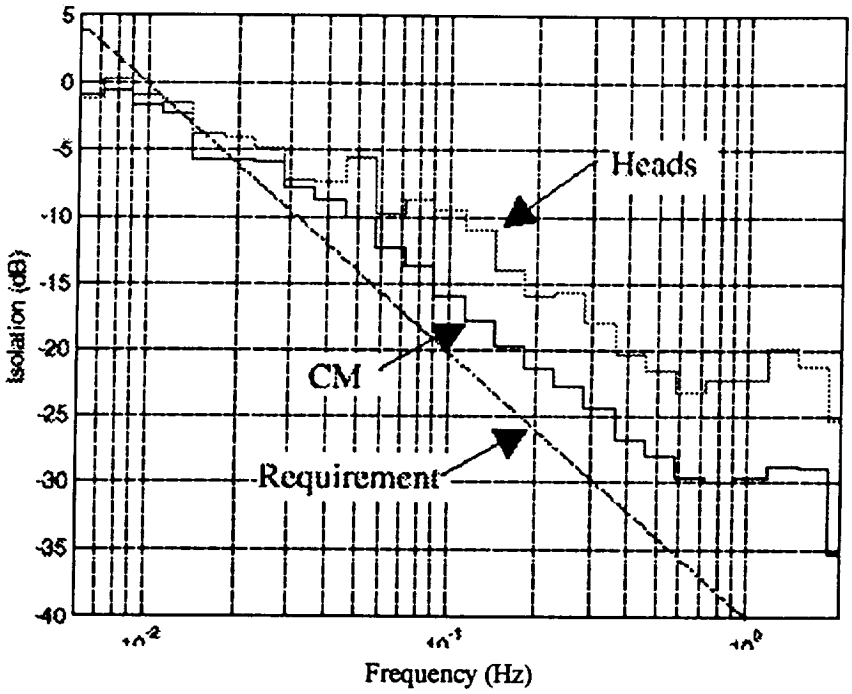

Figure 18: transfer function versus requirement for center-of-mass location and one accelerometer head.